Journal of Solid Mechanics Vol. 9, No. 2 (2017) pp. 351-369

Finite Element Instability Analysis of the Steel Joist of Continuous Composite Beams with Flexible Shear Connectors

H. Bakhshi [1,*], H.R. Ronagh [2]

[1]*Engineering Faculty, Hakim Sabzevari University, Sabzevar, Iran*
[2]*Instiutute for Infrastructure Engineering, Western Sydney University, Penrith, NSW 2751, Australia*

Received 5 March 2017; accepted 4 May 2017

ABSTRACT

Composite steel/concrete beams may buckle in hogging bending regions. As the top flange of I-beam in that arrangement is restricted from any translational deformation and twist, the web will distort during buckling presenting a phenomenon often described as restricted distortional buckling. There are limited studies available in the literature of restricted distortional buckling of composite steel/concrete I-beams subjected to negative or hogging bending. There is none however that includes the effect of partial shear interaction. In this paper, finite element models for in-plane analysis and out-of-plane buckling of continuous composite I-beams including the effects of partial shear interaction are presented.

Keywords : Finite element model; In-plane analysis; Out-of-plane buckling; Restricted distortional buckling; Partial shear interaction.

1 INTRODUCTION

THIS paper discusses the instability of the steel joist of a composite beam composed of a steel I-beam and a concrete slab connected together by shear connectors which is subjected to negative or hogging bending. This is a relatively complicated problem. The instability analysis becomes even more complex when partial shear interaction between steel joist and concrete slab is taken into account. As the top flange of I-beam in that arrangement is restricted from any translational deformation and twist, the web will distort during buckling presenting a phenomenon often described as restricted distortional buckling. If this buckling is prevented, large rotational capacities can be achieved beyond the plastic moment of resistance and advantageous plastic design is feasible. Consequently, the moment redistribution in the hogging region that is possible due to the ductility of such beams is achievable prior to failure and significant economies can be obtained due to that distribution.

The very early work on the concept of imperfect composite action between concrete and steel for composite structures were tests on six simply supported composite steel and concrete T-beams performed by Newmark et al. [1]. Unlike simply-supported composite beams, continuous composite beams are more complex due to concrete cracking in hogging regions. Theoretical studies were published in order to address the problem of the buckling of steel joist of composite beams with both continuously varying axial force and bending moment (Bradford and Gao [2]; Dekker et al. [3]; Tehami [4]; Jasim and Atalla [5]; Nie and Cai [6]; Nie et al. [7]; Ranzi et al. [8]). Bradford and Gao [2] presented a simple method to examine the stability of fixed-ended composite steel-concrete beams taking into account the difference between its sagging and hogging bending rigidities, due to the concrete cracking in

*Corresponding author. Tel.: +98 51 44012785; Fax: +98 51 44012787.
E-mail address: h.bakhshi@hsu.ac.ir (H. Bakhshi).

tension. Bradford [9] developed a rational model for predicting the elastic buckling load of thin-walled I-section columns, restrained fully against translation and elastically against twist at one flange and subjected to a uniformly distributed axial force. Bradford and Ronagh [10] extended the 12 degrees of freedom element developed by Bradford and Trahair [11] to the 16 degrees of freedom element for predicting the distortional buckling of restrained I-section members more accurately. Bradford and Ronagh [12] considered the elastic lateral-distortional buckling of composite cantilevers, whose steel portion was tapered, under moment gradient. Bradford and Ge [13] demonstrated an in-plane analysis of elastic distortional buckling of a two-span continuous I-beam with a concentrated load in each span. It was concluded that the distortional buckling resistance of two-span continuous beams decreased when the concentrated loads within each span were located toward the centre of each span, since the bending moment distribution was more uniform. Bradford and Kemp [14] reviewed the research to date into local and lateral-distortional buckling in the negative moment region of continuous composite beams, and provided design proposals. Vrcelj [15] presented the development of a rational generic model to investigate the elastic restrained distortional buckling of I-section members in both half-through girder bridges and composite tee-beams in hogging regions. Her study, however, only addressed the issue in the light of full interaction analysis. Xu and Wu [16] presented a new plane stress model for the composite beams with interlayer slips using the state space method. Wang and Chung [17] proved that the deformation characteristics of shear connectors are very important in predicting the structural behavior of composite beams with large rectangular web openings. Zona and Ranzi [18] considered the shear deformability of the steel and slab components at various load levels. Chakrabarti et al. [19] proposed a new finite element model based on a higher order beam theory for the analysis of composite beams. The proposed model takes into account the effect of partial shear interaction between the adjacent layers as well as transverse shear deformation of the beams. Lezgy-Nazargah [20] presented an isogeometric approach based on non-uniform rational B-spline (NURBS) basis functions for the analysis of composite steel–concrete beams. Lezgy-Nazargah and Kafi [21] proposed a finite element model for the analysis of composite steel-concrete beams based on a refined high-order theory. The employed theory of these researchers satisfies all the kinematic and stress continuity conditions at the layer interfaces and considers effects of the transverse normal stress and transverse flexibility. He and Yang [22] made comparisons among the classical, Reddy's higher order and plane stress models. They also presented a higher order model for composite beams and verified it through comparison via other models. Chen et al. [23] presented an experimental study of the flexural behavior and shear transfer mechanisms of shallow cellular composite beams where the concrete passing through the steel web opening is combined with a steel tie-bar element to form the shear connection.

In this paper, finite element models for in-plane analysis and out-of-plane buckling of continuous composite I-beams including the effects of partial shear interaction are presented. The first finite element model is developed to investigate the in-plane behavior of composite beams. The model provides the bending moment distribution along the length allowing for the variation in the rigidities of the cross-section in hogging and sagging regions. The stress resultants that act in the steel joist are then used as the input data for the out-of-plane finite element. The out-of-plane finite element model undertakes the out-of-plane distortional buckling analysis of the steel joist. Both of the models and some results are presented in the following.

2 THE IN-PLANE MODEL

In the in-plane finite element formulation, a composite beam is modelled as two one-dimensional beam elements, one for concrete and the other for steel. Each beam has two nodes with three degrees of freedom per node totaling to twelve degrees of freedom for the element (Fig.1(a)). Based on the assumption that the curvature is the same in both elements at the same point along the length due to the lack of transverse separation at the contact interface, displacements and twists can be reduced to eight degrees of freedom as is shown in Fig. 1(b). A new model with two nodes and four degrees of freedom per node is then proposed.

In the first model with twelve degrees of freedom (Fig. 1(a)), the generalized displacements containing these freedoms are presented by the vector q_f as:

$$q_f = \left\{ q_{f1} \;\; q_{f2} \;\; q_{f3} \;\; q_{f4} \;\; q_{f5} \;\; q_{f6} \;\; q_{f7} \;\; q_{f8} \;\; q_{f9} \;\; q_{f10} \;\; q_{f11} \;\; q_{f12} \right\}^T \tag{1}$$

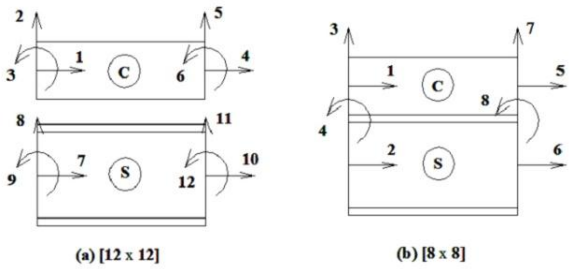

Fig.1
In-plane composite beam finite element.

In the second model with eight degrees of freedom (Fig. 1(b)), the vector q_p can be written as:

$$q_p = \left\{ q_{p1} \;\; q_{p2} \;\; q_{p3} \;\; q_{p4} \;\; q_{p5} \;\; q_{p6} \;\; q_{p7} \;\; q_{p8} \right\}^T \tag{2}$$

Introducing the shape functions

$$N_1 = 1 - \frac{X}{L} \tag{3}$$

$$N_2 = \frac{X}{L} \tag{4}$$

$$N_3 = 1 - \frac{3X^2}{L^2} + \frac{2X^3}{L^3} \tag{5}$$

$$N_4 = x - \frac{2x^2}{L} + \frac{x^3}{L^2} \tag{6}$$

$$N_5 = \frac{3x^2}{L^2} - \frac{2x^3}{L^3} \tag{7}$$

$$N_6 = -\frac{x^2}{L} + \frac{x^3}{L^2} \tag{8}$$

The displacements along the length of the concrete and the steel can be written as:
Axial displacement:

$$u_c = N_1 q_{f1} + N_2 q_{f4} \tag{9}$$

$$u_s = N_1 q_{f7} + N_2 q_{f10} \tag{10}$$

Vertical displacement:

$$v_c = N_3 q_{f2} + N_4 q_{f3} + N_5 q_{f5} + N_6 q_{f6} \tag{11}$$

$$v_s = N_3 q_{f8} + N_4 q_{f9} + N_5 q_{f11} + N_6 q_{f12} \tag{12}$$

Rotation:

$$\theta_c = \frac{dv_c}{dx} = v_c' = N_3' q_{f2} + N_4' q_{f4} + N_5' q_{f5} + N_6' q_{f6} \tag{13}$$

$$\theta_s = \frac{dv_s}{dx} = v_s' = N_3' q_{f8} + N_4' q_{f9} + N_5' q_{f11} + N_6' q_{f12} \tag{14}$$

Having this, the displacements at the shear connector level u_{sc1} and u_{sc2} shown in Fig.2 can be calculated as:

$$u_{sc1} = u_c + h_c \theta_c \tag{15}$$

$$u_{sc2} = u_s - h_s \theta_s \tag{16}$$

The slip is then defined as:

$$s = u_{sc1} - u_{sc2} \tag{17}$$

$$s = u_c - u_s + (h_c \theta_c + h_s \theta_s) \tag{18}$$

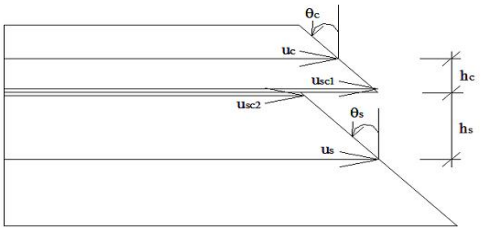

Fig.2
Slip relations of in-plane composite element.

Replacing Eq.(9), (10), (13) and (14) into Eq.(17), we get

$$s = \langle N_1 \;\; h_c \; N_3' \; h_c \; N_4' \; N_2 \; h_c \; N_5' \; h_c \; N_6' - N_1 \; h_s \; N_3' \; h_s \; N_4' - N_2 \; h_s \; N_5' \; h_s \;\; N_6' \rangle q_f \tag{19}$$

or as:

$$S = D_s \; q_f$$

where

$$q_f = \left\{ q_{f1} \; q_{f2} \; q_{f3} \; q_{f4} \; q_{f5} \; q_{f6} \; q_{f7} \; q_{f8} \; q_{f9} \; q_{f10} \; q_{f11} \; q_{f12} \right\}^T$$

$$D_S = N_1 \; h_c \; N_3' \; h_c \; N_4' \; N_2 \; h_c \; N_5' \; h_c \; N_6' - N_1 \; h_s \; N_3' \; h_s \; N_4' - N_2 \; h_s \; N_5' \; h_s \; N_6'$$

and D_S is given in the Appendix.

Stiffness matrix of the composite element is the sum of the stiffness matrices of the concrete, the steel and the shear connector elements. Using the energy approach, the strain-energy of shear connector element is defined as:

$$U_{shear} = \frac{1}{2}\int_0^L k_s \; s^2 \; dx$$

$$U_{shear} = \frac{k_s}{2}\int_0^L q_f^T \; D_s^T \; D_s \; q_f \; dx \tag{20}$$

$$U_{shear} = \frac{1}{2} \; q_f^T \; K_{shear} \; q_f$$

where

$$K_{shear} = k_s \int_0^L D_s^T \; D_s \; dx \tag{21}$$

Is identified as the stiffness matrix of the shear connector element. The stiffness matrix K_{cs} of the concrete and the steel is developed from the basic stiffness matrix of beam element. The total stiffness of composite element is thus obtained from

$$U = \frac{1}{2} q_f^T \; K_f \; q_f \tag{22}$$

where

$$K_f = K_{shear} + K_{cs} \tag{23}$$

On the other hand, a relation between the displacements of the element with twelve degrees of freedom and the element with eight degrees of freedom in Fig. 1 can be expressed as:

$$q_f = H \; q_p \tag{24}$$

In which H is given in the Appendix.
Eq. (23) can be rewritten as:

$$U = \frac{1}{2} q_f^T \; K_f \qquad\qquad q_f = \frac{1}{2} q_p^T \; K_p \; q_p \tag{25}$$

where

$$K_p = H^T \; k_f \; H \tag{26}$$

Is identified as the total stiffness matrix of the composite element with eight degrees of freedom. A finite element program called PARTIALSHEAR is then compiled to produce the slip, the lateral displacements and twist of the concrete and the steel, and the stress resultants of steel joist. These will be used as input for the out-of-plane buckling investigation performed by the out-of-plane finite element.

As the elements work with fixed properties along the length, the sagging and hogging properties may need to be defined based on the position of the contra flexure point. Since this position is unknown in prior, trial and error based analysis needs to be carried out to find its location. The analysis therefore starts with a set number of elements at set lengths. The lengths of elements neighboring the contra flexure point are then adjusted to allow the zero bending point to occur exactly at their junction. The process of adjustment continues until the point of contra flexure remains at the assumed position within an acceptable error range.

3 THE OUT-OF-PLANE MODEL

The geometry of the beam-column element and the *x-y-z* Cartesian axis system are defined as shown in Fig.3. The element is a prismatic I-girder with flange width b_f, flange thickness t_f , web depth h_w , and web thickness t_w . Lateral displacement u and twist θ of the top and the bottom of the web along the length z are used to define the shape of the beam during buckling. The subscripts T and B refer to the top and bottom flanges, respectively. Due to the restraint provided through the shear connectors to the concrete slab, the displacements at the top flange of I-girder are assumed to be zero.

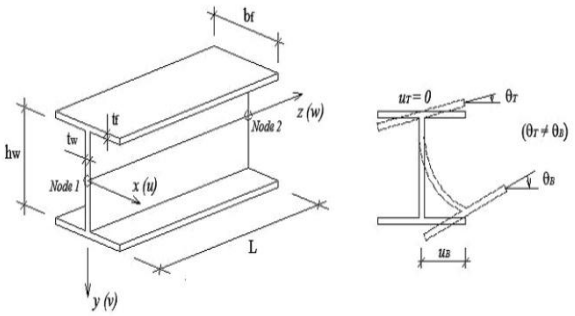

Fig.3
The beam element and its displacements.

The element is considered to be subjected to end moments M_0 and M_L , end axial forces N_0 and N_L , and end shear forces V_0 and V_L in the manner shown in Fig. 4.

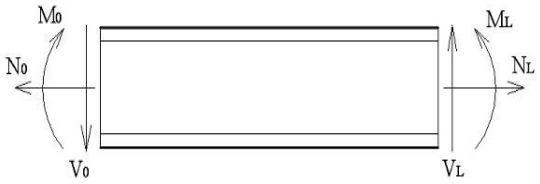

Fig.4
Configuration of element in loading.

The bending moment and axial force are assumed to vary linearly along the length of the element, so that

$$M = M_0\left(1-\frac{z}{L}\right)+M_L\left(\frac{z}{L}\right) \tag{27}$$

$$N = N_0\left(1-\frac{z}{L}\right)+N_L\left(\frac{z}{L}\right) \tag{28}$$

The shears are equal and can be obtained from static's equilibrium as:

$$V_0 = V_L = \frac{M_0 - M_L}{L} \tag{29}$$

In the *z*-direction, the buckled shape is represented by the lateral and twist displacements of the flanges, u_B, θ_T and θ_B . All these deflections and twists are defined as cubic polynomials along the length. The flanges' displacements are therefore given as:

$$u_B = \alpha_1 L + \alpha_2 z + \alpha_3 \frac{z^2}{L} + \alpha_4 \frac{z^3}{L^2} \tag{30}$$

$$\theta_T = \alpha_5 + \alpha_6 \frac{z}{L} + \alpha_7 \frac{z^2}{L^2} + \alpha_8 \frac{z^3}{L^3} \tag{31}$$

$$\theta_B = \alpha_9 + \alpha_{10} \frac{z}{L} + \alpha_{11} \frac{z^2}{L^2} + \alpha_{12} \frac{z^3}{L^3} \tag{32}$$

which can be written in the matrix form as:

$$u = \left\{ u_B \;\; \theta_T \;\; \theta_B \right\}^T \tag{33}$$

$$M_1 = \left\{ L \;\; z \;\; \frac{z^2}{L} \;\; \frac{z^3}{L^2} \right\} \tag{34}$$

$$M_2 = \left\{ 1 \;\; \frac{z}{L} \;\; \frac{z^2}{L^2} \;\; \frac{z^3}{L^3} \right\} \tag{35}$$

$$M_2 = \begin{Bmatrix} M_1 & 0 & 0 \\ 0 & M_2 & 0 \\ 0 & 0 & M_2 \end{Bmatrix} \tag{36}$$

or as:

$$u = M \;\; \alpha \tag{37}$$

where

$$\alpha = \left\{ \alpha_1, \alpha_2, ..., \alpha_{12} \right\}^T \tag{38}$$

In the *y*-direction, the buckling deformation of the web is also defined by cubic polynomials linking from the top to the bottom of the web. The deflection of any web point in the cross-section can then be expressed as:

$$u_w = \alpha_{13} h_w + \alpha_{14} y + \alpha_{15} \frac{y^2}{h_w} + \alpha_{16} \frac{y^3}{h_w^2} \tag{39}$$

or

$$u_w = H_w^T \;\; \alpha_w \tag{40}$$

where

$$H_w^T = \left\{ h_w \;\; y \;\; \frac{y^2}{h_w} \;\; \frac{y^3}{h_w^2} \right\} \tag{41}$$

$$\alpha_w = \left\{ \alpha_{13} \;\; \alpha_{14} \;\; \alpha_{15} \;\; \alpha_{16} \right\}^T \tag{42}$$

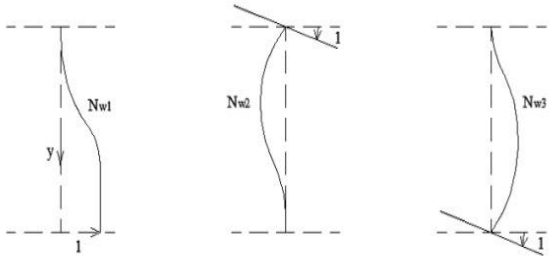

Fig.5
Web element shape function.

The displacement variation of web element shown in Fig. 5 can also be expressed in natural coordinates as:

$$u_w = N_{w1} u_B + N_{w2} \theta_T + N_{w3} \theta_B \tag{43}$$

where

$$N_{w1} = \frac{1}{2} + \frac{3y}{2h_w} - \frac{2y^3}{h_w^3} \tag{44}$$

$$N_{w2} = -\frac{h_w}{8} + \frac{y}{4} + \frac{y^2}{2h_w} - \frac{y^3}{h_w^2} \tag{45}$$

$$N_{w3} = \frac{h_w}{8} + \frac{y}{4} - \frac{y^2}{2h_w} - \frac{y^3}{h_w^2} \tag{46}$$

Eq.(43) can be written as:

$$u_w = N_{w1}\ N_{w2}\ N_{w3}\ u \tag{47}$$

where

$$u = \left\{ u_B \ \ \theta_T \ \ \theta_B \right\}^T \tag{48}$$

and from Eq.(37): $u = M \ \ \alpha$

Hence, Eq. (47) becomes

$$u_w = N_{w1} N_{w2} N_{w3} M \ \ \alpha \tag{49}$$

or

$$u_w = N_w^T \ \ \alpha \tag{50}$$

where

$$N_w^T = N_{w1} N_{w2} N_{w3} M \tag{51}$$

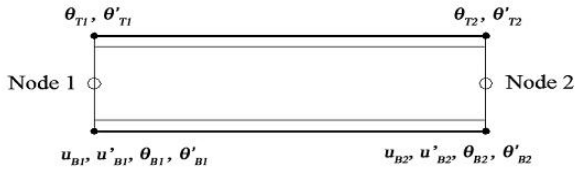

Fig.6
Buckling displacements *q*.

Generalized buckling displacements used are shown in Fig. 6. A prime (') denotes differentiation with respect to *z*. The vector *q* containing these freedoms is written as:

$$q = \{u_{B1}, u'_{B1}, \theta_{T1}, \theta'_{T1}, \theta_{B1}, \theta'_{B1}, u_{B2}, u'_{B2}, \theta_{T2}, \theta'_{T2}, \theta_{B2}, \theta'_{B2}\}^T \tag{52}$$

The generalized buckling displacements q are related to the natural coordinate system α. The relation can be easily obtained by looking at the shape functions at the boundaries. This relation can be expressed as:

$$q = C\ \alpha \tag{53}$$

where the matrix C is a matrix of order 12 and is given in Appendix. Eq.(53) can then be rewritten with the inverse of the matrix C as:

$$\alpha = C^{-1}\ q \tag{54}$$

In a similar manner, buckling displacements u are related to the generalized displacement system q by substituting Eq.(54) into Eq.(37). This gives:

$$u = M\ \ C^{-1}\ q \tag{55}$$

where C^{-1} is given in Appendix.

3.1 Derivation of the stiffness matrix

In order to derive the stiffness matrix using an energy approach, it is necessary to calculate the total energy stored in the beam during buckling. The beam elements representing the flanges and the plate element representing the web would deflect sideways and twist. The strain energy stored can be expressed as:

$$U = U_{fu} + U_{f\theta} + U_w \tag{56}$$

where U_{fu} is the energy associated with the bending of flanges about their major axis, $U_{f\theta}$ is the energy associated with the twist of flanges and bending about their minor axis, and U_w is the strain energy associated with the bending and twisting of the web as a plate.

These energy components can be calculated as:

$$U_{fu} = \frac{1}{2}\int_0^L E_s I_{yf} \left(u''_B\right)^2 dz \tag{57}$$

$$U_{f\theta} = \frac{1}{2}\int_0^L \int_{-\frac{b_f}{2}}^{\frac{b_f}{2}} D_f \left\{ \left(v''_T\right)^2 + \left(v''_B\right)^2 + 2(1-\nu)\left[\left(\frac{\partial^2 v_T}{\partial x\, \partial z}\right)^2 + \left(\frac{\partial^2 v_B}{\partial x\, \partial z}\right)^2 \right] \right\} dx\, dz \tag{58}$$

$$U_w = \frac{1}{2}\int_0^L \int_{-\frac{h_w}{2}}^{\frac{h_w}{2}} \varepsilon^T \ \sigma \ dy \ dz \tag{59}$$

$U_{f\theta}$ is composed of two components, the first component

$$U_{f\theta} = \frac{1}{2}\int_0^L \int_{-\frac{b_f}{2}}^{\frac{b_f}{2}} D_f \left[\left(v_T''\right)^2 + \left(v_B''\right)^2 \right] dx dz \tag{60}$$

Is associated with the bending of flanges about their minor axis.The second component of $U_{f\theta}$ is equal to

$$U_{f\theta} = \frac{1}{2}\int_0^L \int_{-\frac{b_f}{2}}^{\frac{b_f}{2}} 2D_f \ (1-\nu) \left[\left(\frac{\partial^2 v_T}{\partial x \, \partial z} \right)^2 + \left(\frac{\partial^2 v_B}{\partial x \, \partial z} \right)^2 \right] dx dz \tag{61}$$

and is associated with the twist of the flanges.

Since the flanges are assumed to remain rigid, the vertical (*y*-direction) displacement of the flanges can be expressed as:

$$v_T = x \, \theta_T \tag{62}$$

$$v_B = x \, \theta_B \tag{63}$$

Substituting Eqs.(62-63) into Eq.(60) and then integrating over the width of the flanges shows that this component contains the usual twisting terms of the Saint Venant linear torsion as:

$$\frac{1}{2}\int_0^L GJ_f \left[\left(\theta_T'\right)^2 + \left(\theta_B'\right)^2 \right] dz \tag{64}$$

where *G* is the shear modulus equal to:

$$G = \frac{E_s}{2(1+\nu)} \tag{65}$$

and J_f is the torsional rigidity of each flange, which is equal to:

$$J_f = \frac{b_f t_f^3}{3} \tag{66}$$

Hence, $U_{f\theta}$ can be rewritten as:

$$U_{f\theta} = \frac{1}{2}\int_0^L \int_{-\frac{b_f}{2}}^{\frac{b_f}{2}} D_f \left[\left(v_T''\right)^2 + \left(v_B''\right)^2 \right] dx dz + \frac{1}{2}\int_0^L GJ_f \left[\frac{1}{2}\left(\theta_T'\right)^2 + \left(\theta_B'\right)^2 \right] dz \tag{67}$$

The term I_{yf} is the second moment of area of each flange about the *y*-axis, which is equal to:

$$I_{yf} = \frac{b_f^3 t_f}{12} \tag{68}$$

The parameter D_f represents the plate rigidity of flanges and is given by

$$D_f = \frac{E_s t_f^3}{12(1-v^2)} \tag{69}$$

As the web is considered a plate, the generalized strain and stress vector of Eq.(59) can be written as:

$$\varepsilon^T = \left\{ \frac{-\partial^2 u_w}{\partial y^2} \quad \frac{-\partial^2 u_w}{\partial z^2} \quad \frac{2\partial^2 u_w}{\partial y \partial z} \right\} \tag{70}$$

$$\sigma = D_w \begin{bmatrix} 1 & v & 0 \\ v & 1 & 0 \\ 0 & 0 & \frac{1-v}{2} \end{bmatrix} \varepsilon = \frac{E_s t_w^3}{12(1-v^2)} \begin{bmatrix} 1 & v & 0 \\ v & 1 & 0 \\ 0 & 0 & \frac{1-v}{2} \end{bmatrix} \varepsilon \tag{71}$$

where

$$D_w \ \frac{E_s t_w^3}{12(1-v^2)} \tag{72}$$

From Eqs. (54):

$$\alpha = C^{-1} q \tag{73}$$

Therefore:

$$\alpha^T = q^T \ C^{-T} \tag{74}$$

Using Eqs. (57-59), the strain energy equation can be mathematically manipulated to produce

$$U = \frac{1}{2} \alpha^T \ K^a \ \alpha \tag{75}$$

Substituting α and α^T from Eqs.(54, 74) into Eq.(75) we obtain

$$U = \frac{1}{2} q^T \ C^{-T} \ K^\alpha \ C^{-1} \qquad q = \frac{1}{2} q^T \ K \ q \tag{76}$$

From which

$$K = C^{-T} \ K^\alpha \ C^{-1} \tag{77}$$

Is identified as the stiffness matrix of the element.

3.2 Derivation of the stability matrix

The stability matrix relates to the work done by the surface tractions or the loss of the potential energy of the stresses. This loss of potential energy can be written as:

$$W = W_{fu} + W_{f\theta} + W_w \tag{78}$$

where W_{fu} the work is associated with the bending of flanges about their major axis, $W_{f\theta}$ is the work associated with the twist of flanges and bending about their minor axis, and W_w is the work associated with the bending of the web as a plate.

$$W_{fu} = \frac{1}{2}\int_0^L A_f \sigma_B \left(u'_B\right)^2 dz \tag{79}$$

$$W_{f\theta} = \frac{1}{2}\int_0^L \int_{-\frac{b_f}{2}}^{\frac{b_f}{2}} t_f \left[\sigma_T \left(v'_T\right)^2 + \sigma_B \left(v'_B\right)^2\right] dx dz \tag{80}$$

$$W_w = \frac{1}{2}\int_0^L \int_{-\frac{h_w}{2}}^{\frac{h_w}{2}} t_w \begin{bmatrix} \partial u_w / \partial z \\ \partial u_w / \partial y \end{bmatrix}^T \begin{bmatrix} \sigma & \tau \\ \tau & 0 \end{bmatrix} \begin{Bmatrix} \partial u_w / \partial z \\ \partial u_w / \partial y \end{Bmatrix} dy dz \tag{81}$$

In which A_f is the area of each flange and I_{yf} is the second moment of area of each flange about the *y*-axis.

The terms σ and τ represent the stresses along the web obtained in the usual way as:

$$\sigma = \frac{N}{A_x} + \frac{My}{I_x} \tag{82}$$

$$\tau = -\frac{v}{h_w t_w} \tag{83}$$

where $V = \frac{M_0 - M_L}{L}$ from Eq.(29). The terms σ_T and σ_B the stresses at the top and bottom flanges, are calculated as:

$$\sigma_T = \frac{N}{A_x} - \frac{Mh_w}{2I_x} \tag{84}$$

$$\sigma_B = \frac{N}{A_x} + \frac{Mh_w}{2I_x} \tag{85}$$

In the matrix form, the work done by the surface tractions or the loss of the potential energy of the stresses becomes

$$W = \frac{1}{2}\ \alpha^T\ S^a\ \alpha \tag{86}$$

Similar to Eq.(75), Eq.(86) has to be derived in terms of the generalized displacement q. Using Eqs. (54, 74), this transformation can be performed as:

$$W = \frac{1}{2}\ q^T\ C^{-T}\ S^{\alpha}\ C^{-1} \qquad q = \frac{1}{2}\ q^T\ S\ q \tag{87}$$

where

$$S = C^{-T}\ S^{\alpha}\ C^{-1} \tag{88}$$

Is identified as the stability matrix of the element.

3.3 Buckling solution

The global stiffness and stability matrices of the structure are calculated by assembling the stiffness and stability matrices of all members. The buckling load factor λ can be found using an eigen technique that can solve the linear non-standard eigen problem of

$$(K - \lambda S)q_g = 0 \tag{89}$$

where K and S are the assembled stiffness and stability matrices and q_g is the global buckling degrees of freedom. The solution of Eq. (89) for nontrivial q_g is a standard eigen problem, and is solved herein for the buckling load factor λ and buckling mode shape or eigenvector q_g .

In order to minimise the numerical efforts, the stiffness and stability matrices, K and S, are derived symbolically as much as possible. Here, the stiffness and stability matrices are calculated symbolically using MATHEMATICA. The elements of these matrices are then input into a finite element program called FED12 written in FORTRAN. This program processes the input of the elements, calculates the matrices, solves for the eigenvalue and provides the associated eigen modes.

4 EXAMPLES

A standard two-span continuous composite I-beam, 10m in span-length subjected to 50 *KN/m* uniformly distributed load is considered. Cross-sectional dimensions of the beam are $E_c = 32{,}000 N/mm^2, E_s = 200{,}000 N/mm^2$, $h = 1{,}000mm, b_f = 400mm, t_f = 28mm, t_w = 16mm$. The concrete slab dimensions are $2{,}500mm \times 150mm$ and the reinforcement ratio (A_r/A_c) is set at 1.8%.

Figs. 7, 8 and Fig. 9 contain the results of the in-plane analysis for various degrees of interaction. The stress resultants of steel joist are then used as the input data for the out-of-plane buckling investigation. The in-plane bending moment of steel joist in hogging region is larger for beams with a lower degree of interaction. These beams are therefore more susceptible to out-of-plane buckling.

As is seen in Table 1., the partial interaction design has affected the buckling resistance of the beam. The buckling mode shapes have minor influences due to partial shear interaction and are illustrated in Fig. 10 and Fig. 11.

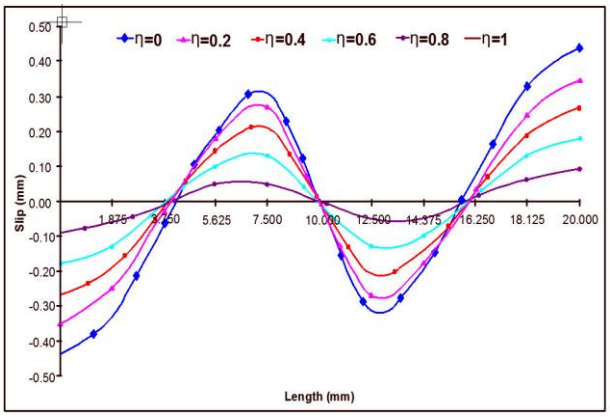

Fig.7
Slip of continuous composite beam.

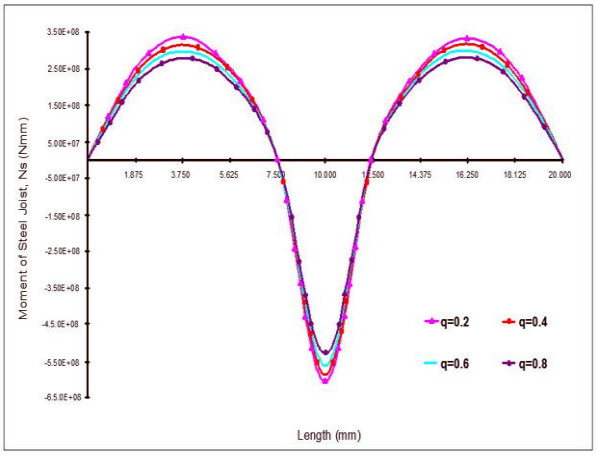

Fig.8
In-plane bending moment of steel joist.

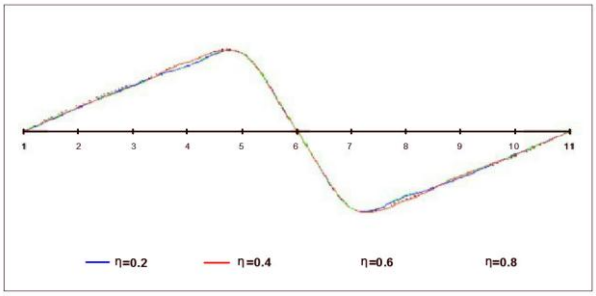

Fig.9
In-plane axial force of steel joist.

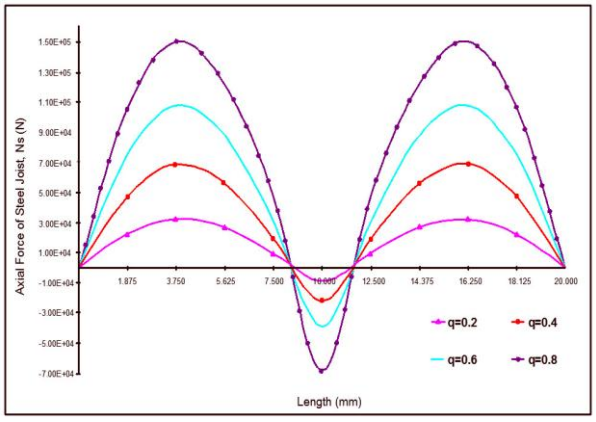

Fig.10
Lateral displacement of bottom flange along the length.

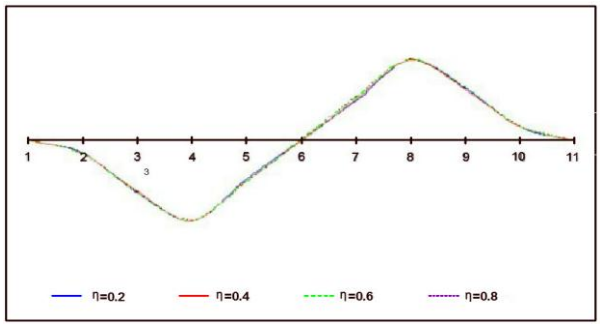

Fig.11
Buckling twist of bottom flange along the length.

Table 1
Partial interaction (PI) effects on critical buckling load.

Degree of Interaction (η)	Critical Buckling Load $w_{cr}(KN/m)$	PI Effects $\left\|\frac{w_{cr,PI}-w_{cr,FI}}{w_{cr,FI}}\times 100\right\|_{(\%)}$
0.2	2,252	15.4
0.4	2,350	11.8
0.6	2,466	7.4
0.8	2,592	2.7
1.0	2,663	0.0

5 CONCLUSIONS

The finite element models for analyzing the in-plane analysis and out-of-plane restricted distortional buckling of continuous composite I-beams including the effects of partial shear interaction are presented. The proposed models can be used effectively to account for the differences in the beam's flexural rigidities in hogging and sagging regions due to the concrete cracking in tension. These versatile models are capable of accommodating different types of boundary and loading conditions. They can be used to develop more economical and efficient designs.

The example presented shows that the two-span continuous composite I-beam is more prone to buckling at lower degrees of interaction. Since the degree of interaction affects the buckling resistance of steel joist, the partial interaction design is found to be critical in terms of strength and stability of continuous composite I-beams subjected to uniformly distributed loads.

APPENDIX

The degree of interaction, η, is defined in this paper as 1 minus the ratio of the slip at the steel/concrete interface in a shear span with partial interaction to the slip in case of no-interaction. η Varies from 0 (no-interaction) to 1 (full-interaction). The relation for the degree of interaction can be written as:

$$\eta = 1 - \frac{S_x}{S_{ni,x}}$$

where S_x is the slip at position *x* of the steel/concrete interface of composite beam with partial interaction (with any k_s as the stiffness of the shear connectors); $S_{ni,x}$ is the slip at position *x* of the steel/concrete interface of composite beam with no-interaction (with $k_s = 0$). Often *x* is chosen at the location of maximum slip.

The matrices developed in the finite element models can be presented in the following.

$$D_s = \left\{ d_{s1}\ d_{s2}\ d_{s3}\ d_{s4}\ d_{s5}\ d_{s6}\ d_{s7}\ d_{s8}\ d_{s9}\ d_{s10}\ d_{s11}\ d_{s12} \right\}$$

$$d_{s1}=1-\frac{x}{L} \qquad d_{s2}=-\frac{6h_c x}{L^2}+\frac{6h_c x^2}{L^3} \qquad d_{s3}=h_c-\frac{4h_c x}{L}+\frac{3h_c x^2}{L^2}$$

$$d_{s4}=\frac{x}{L} \qquad d_{s5}=\frac{6h_c x}{L^2}-\frac{6h_c x^2}{L^3} \qquad d_{s6}=-\frac{2h_c x}{L}+\frac{3h_c x^2}{L^2}$$

$$d_{s7}=\frac{x}{L}-1 \qquad d_{s8}=-\frac{6h_s x}{L^2}+\frac{6h_s x^2}{L^3} \qquad d_{s9}=h_s-\frac{4h_s x}{L}+\frac{3h_s x^2}{L^2}$$

$$d_{s10}=-\frac{x}{L} \qquad d_{s11}=\frac{6h_s x}{L^2}-\frac{6h_s x^2}{L^3} \qquad d_{s12}=-\frac{2h_s x}{L}+\frac{3h_s x^2}{L^2}$$

The matrices H and H^T are defined as:

$$H^T=\begin{bmatrix}1&0&0&0&0&0&0&0&0&0&0&0\\0&0&0&0&0&0&1&0&0&0&0&0\\0&1&0&0&0&0&0&1&0&0&0&0\\0&0&1&0&0&0&0&0&1&0&0&0\\0&0&0&1&0&0&0&0&0&0&0&0\\0&0&0&0&0&0&0&0&0&1&0&0\\0&0&0&0&1&0&0&0&0&0&1&0\\0&0&0&0&0&1&0&0&0&0&0&1\end{bmatrix} \qquad H=\begin{bmatrix}1&0&0&0&0&0&0&0\\0&0&1&0&0&0&0&0\\0&0&0&1&0&0&0&0\\0&0&0&0&1&0&0&0\\0&0&0&0&0&0&1&0\\0&0&0&0&0&0&0&1\\0&1&0&0&0&0&0&0\\0&0&1&0&0&0&0&0\\0&0&0&1&0&0&0&0\\0&0&0&0&0&1&0&0\\0&0&0&0&0&0&1&0\\0&0&0&0&0&0&0&1\end{bmatrix}$$

The transformation matrices C and C^{-1} are given as follows:

$$C=\begin{bmatrix}C_{u0}&0&0\\0&C_{\theta 0}&0\\0&0&C_{\theta 0}\\C_{uL}&0&0\\0&C_{\theta L}&0\\0&0&C_{\theta L}\end{bmatrix}$$

where:

$$C_{u0}=\begin{bmatrix}L&0&0&0\\0&1&0&0\end{bmatrix} \qquad C_{\theta 0}=\begin{bmatrix}1&0&0&0\\0&\frac{1}{L}&0&0\end{bmatrix}$$

$$C_{uL}=\begin{bmatrix}L&L&L&L\\0&1&2&3\end{bmatrix} \qquad C_{\theta L}=\begin{bmatrix}1&1&1&1\\0&\frac{1}{L}&\frac{2}{L}&\frac{3}{L}\end{bmatrix}$$

$$C = \begin{bmatrix}
L & 0 & 0 & 0 & 0 & 0 & 0 & 0 & 0 & 0 & 0 & 0 \\
0 & 1 & 0 & 0 & 0 & 0 & 0 & 0 & 0 & 0 & 0 & 0 \\
0 & 0 & 0 & 0 & 1 & 0 & 0 & 0 & 0 & 0 & 0 & 0 \\
0 & 0 & 0 & 0 & 0 & \frac{1}{L} & 0 & 0 & 0 & 0 & 0 & 0 \\
0 & 0 & 0 & 0 & 0 & 0 & 0 & 0 & 1 & 0 & 0 & 0 \\
0 & 0 & 0 & 0 & 0 & 0 & 0 & 0 & 0 & \frac{1}{L} & 0 & 0 \\
L & L & L & L & 0 & 0 & 0 & 0 & 0 & 0 & 0 & 0 \\
0 & 1 & 2 & 3 & 0 & 0 & 0 & 0 & 0 & 0 & 0 & 0 \\
0 & 0 & 0 & 0 & 1 & 1 & 1 & 1 & 0 & 0 & 0 & 0 \\
0 & 0 & 0 & 0 & 0 & \frac{1}{L} & \frac{2}{L} & \frac{3}{L} & 0 & 0 & 0 & 0 \\
0 & 0 & 0 & 0 & 0 & 0 & 0 & 0 & 1 & 1 & 1 & 1 \\
0 & 0 & 0 & 0 & 0 & 0 & 0 & 0 & 0 & \frac{1}{L} & \frac{2}{L} & \frac{3}{L}
\end{bmatrix}$$

$$C^{-1} = \begin{bmatrix}
\frac{1}{L} & 0 & 0 & 0 & 0 & 0 & 0 & 0 & 0 & 0 & 0 & 0 \\
0 & 1 & 0 & 0 & 0 & 0 & 0 & 0 & 0 & 0 & 0 & 0 \\
\frac{-3}{L} & -2 & 0 & 0 & 0 & 0 & \frac{3}{L} & -1 & 0 & 0 & 0 & 0 \\
\frac{2}{L} & 1 & 0 & 0 & 0 & 0 & \frac{-2}{L} & 1 & 0 & 0 & 0 & 0 \\
0 & 0 & 1 & 0 & 0 & 0 & 0 & 0 & 0 & 0 & 0 & 0 \\
0 & 0 & 0 & L & 0 & 0 & 0 & 0 & 0 & 0 & 0 & 0 \\
0 & 0 & -3 & -2L & 0 & 0 & 0 & 0 & 3 & -L & 0 & 0 \\
0 & 0 & 2 & L & 0 & 0 & 0 & 0 & -2 & L & 0 & 0 \\
0 & 0 & 0 & 0 & 1 & 0 & 0 & 0 & 0 & 0 & 0 & 0 \\
0 & 0 & 0 & 0 & 0 & L & 0 & 0 & 0 & 0 & 0 & 0 \\
0 & 0 & 0 & 0 & -3 & -2L & 0 & 0 & 0 & 0 & 3 & -L \\
0 & 0 & 0 & 0 & 2 & L & 0 & 0 & 0 & 0 & -2 & L
\end{bmatrix}$$

The web displacement matrix is given as follows:

$$N_w^T = \begin{bmatrix} L\left(\frac{1}{2}+\frac{3y}{2h_w}-\frac{2y^3}{h_w^3}\right) \\ \left(\frac{1}{2}+\frac{3y}{2h_w}-\frac{2y^3}{h_w^3}\right)z \\ \left(\frac{1}{2}+\frac{3y}{2h_w}-\frac{2y^3}{h_w^3}\right)\frac{z^2}{L} \\ \left(\frac{1}{2}+\frac{3y}{2h_w}-\frac{2y^3}{h_w^3}\right)\frac{z^3}{L^2} \\ -\frac{h_w}{8}+\frac{y}{4}+\frac{y^2}{2h_w}-\frac{y^3}{h_w^2} \\ \left(-\frac{h_w}{8}+\frac{y}{4}+\frac{y^2}{2h_w}-\frac{y^3}{h_w^2}\right)\frac{z}{L} \\ \left(-\frac{h_w}{8}+\frac{y}{4}+\frac{y^2}{2h_w}-\frac{y^3}{h_w^2}\right)\frac{z^2}{L^2} \\ \left(-\frac{h_w}{8}+\frac{y}{4}+\frac{y^2}{2h_w}-\frac{y^3}{h_w^2}\right)\frac{z^3}{L^3} \\ \frac{h_w}{8}+\frac{y}{4}-\frac{y^2}{2h_w}-\frac{y^3}{h_w^2} \\ \left(\frac{h_w}{8}+\frac{y}{4}-\frac{y^2}{2h_w}-\frac{y^3}{h_w^2}\right)\frac{z}{L} \\ \left(\frac{h_w}{8}+\frac{y}{4}-\frac{y^2}{2h_w}-\frac{y^3}{h_w^2}\right)\frac{z^2}{L^2} \\ \left(\frac{h_w}{8}+\frac{y}{4}-\frac{y^2}{2h_w}-\frac{y^3}{h_w^2}\right)\frac{z^3}{L^3} \end{bmatrix}$$

REFERENCES

[1] Newmark N.M., 1951, Test and analysis of composite beams with incomplete interaction, *Proceedings of Society for Experimental Stress Analysis* **9**(1): 75-92.

[2] Bradford M.A., Gao Z.,1992, Distortional buckling solutions for continuous composite beams, *Journal of Structural Engineering* **118**(1): 73-89.

[3] Dekker N.W., 1995, Factors influencing the strength of continuous composite beams in negative bending, *Journal of Constructional Steel Research* **34**: 161-185.

[4] Tehami M.,1997, Local buckling in class 2 continuous composite beams, *Journal of Constructional Steel Research* **43**(1-3): 141-159.

[5] Jasim N.A., Atalla A., 1999, Deflections of partially composite continuous beams: A simple approach, *Journal of Constructional Steel Research* **49**: 291-301.

[6] Nie J., Cai C.S., 2003, Steel-concrete composite beams considering shear slip effects, *Journal of Structural Engineering* **129**(4): 495-506.

[7] Nie J., Fan J., Cai C. S., 2004, Stiffness and deflection of steel-concrete composite beams under negative bending, *Journal of Structural Engineering* **130**(11): 1842-1851.

[8] Ranzi G., Bradford M.A., Uy B., 2004, A direct stiffness analysis of a composite beam with partial interaction, *International Journal for Numerical Methods in Engineering* **61**: 657-672.

[9] Bradford M.A., 1997, Lateral-distortional buckling of continuously restrained columns, *Journal of Constructional Steel Research* **42**(2): 121-139.

[10] Bradford M.A., Ronagh H.R., 1997, Generalized elastic buckling of restrained I-beams by FEM, *Journal of Structural Engineering* **23**(12): 1631-1637.

[11] Bradford M.A., Trahair N.S., 1981, Distortional buckling of I-beams, *Journal of The Structural Division* **107**: 355-370.

[12] Bradford M.A., Ronagh H.R., 1997, Elastic distortional buckling of tapered composite beams, *Journal of Structural Engineering and Mechanics* **5**(3): 269-281.
[13] Bradford M.A., Ge X.P., 1997, Elastic distortional buckling of continuous I-beams, *Journal of Constructional Steel Research* **41**(2-3): 249-266.
[14] Bradford M.A., Kemp A.R., 2000, Buckling in continuous composite beams, *Progress in Structural Engineering and Materials* **2**: 169-178.
[15] Vrcelj Z., 2004, *Buckling Modes in Continuous Composite Beams*, PhD Thesis, The University of New South Wales, Sydney, Australia.
[16] Xu R., Wu Y.F.,2007, Two-dimensional analytical solutions of simply supported composite beams with interlayer slips, *International Journal of Solids and Structures* **44**: 165-175.
[17] Wang A.J., Chung K.F., 2008, Advanced finite element modelling of perforated composite beams with flexible shear connectors, *Engineering Structures* **30**(10): 2724-2738.
[18] Zona A., Ranzi G., 2011, Finite element models for non-linear analysis of steel concrete composite beams with partial interaction in combined bending and shear, *Finite Element in Analysis and Design* **47**(2): 98-118.
[19] Chakrabarti A., Sheikh A.H., Griffith M., Oehlers D.J., 2012, Analysis of composite beams with partial shear interactions using a higher order beam theory, *Engineering Structur* **36**: 283-291.
[20] Lezgy-Nazargah M., 2014, An isogeometric approach for the analysis of composite steel–concrete beams, *Thin-Walled Structures* **84**: 406-415.
[21] Lezgy-Nazargah M., Kafi L., 2015, Analysis of composite steel-concrete beams using a refined high-order beam theory, *Steel and Composite Structures* **18**(6): 1353-1368.
[22] He G., Yang X., 2015, Dynamic analysis of two-layer composite beams with partial interaction using a higher order beam theory, *International Journal of Mechanical Sciences* **90**: 102-112.
[23] Chen S., Limazie T., Tan J., 2015, Flexural behavior of shallow cellular composite floor beams with innovative shear connections, *Journal of Constructional Steel Research* **106**: 329-346.